

# Fabrication of NiO Nanoparticle-Coated Lead Zirconate Titanate Powders by the Heterogeneous Precipitation Method

Ping-Hua Xiang, Xian-Lin Dong, Chu-De Feng, and Yong-Ling Wang

Shanghai Institute of Ceramics, Chinese Academy of Sciences, Shanghai 200050, P.R. China

**NiO nanoparticle-coated lead zirconate titanate (PZT) powders are successfully fabricated by the heterogeneous precipitation method using PZT, Ni(NO<sub>3</sub>)<sub>2</sub>·6H<sub>2</sub>O, and NH<sub>4</sub>HCO<sub>3</sub> as the starting materials. The amorphous NiCO<sub>3</sub>·2Ni(OH)<sub>2</sub>·2H<sub>2</sub>O are uniformly coated on the surface of PZT particles. XRD analysis and the selected-area diffraction (SAD) pattern indicate that the amorphous coating layer is crystallized to NiO after being calcined at 400°C for 2 h. TEM images show that the NiO particles of ~8 nm are spherical and weakly agglomerated. The thickness of the nanocrystalline NiO coating layer on the surface of PZT particle is ~30 nm.**

## I. Introduction

LEAD zirconate titanate, Pb(Zr<sub>x</sub>Ti<sub>1-x</sub>)O<sub>3</sub> (PZT), and related ceramics are widely used in applications such as pressure sensors, ultrasonic motors, and stack-type actuators because of their excellent piezoelectric properties. However, their poor mechanical and electrical reliability are critical limitations on the high-powered applications of these devices.<sup>1,2</sup> Therefore, improving the mechanical properties and electrical reliability of PZT-based materials has been intensely investigated in recent years. Incorporating submicrometer- and nanosized second-phase (platinum, silver, MgO, and Al<sub>2</sub>O<sub>3</sub>) in the brittle PZT ceramic matrix has been found to be a promising way to improve their mechanical properties and electrical reliability.<sup>3–6</sup> Because of the grain-size reduction and the matrix grain boundaries reinforcement from adding MgO nanoparticles, the fracture strength of a PZT/MgO composite is 1.7 times higher than that of commercially available PZT. The PZT/Al<sub>2</sub>O<sub>3</sub> composite showed excellent electrical durability and fatigue resistance, owing to the microcrack pinned by Al<sub>2</sub>O<sub>3</sub> particles at the boundaries in the composites. For PZT materials, NiO-like MgO and Al<sub>2</sub>O<sub>3</sub> are known to belong to acceptor additives and thus the PZT nanocomposite incorporating NiO nanoparticles may obtain high mechanical properties and excellent durability. The reinforcement mechanisms show the importance of homogeneity and fine size of the second inclusion.<sup>7,8</sup> However, it is difficult to control the microstructure of a PZT nanocomposite by conventional techniques involving the mechanical mixing of ceramic powders and nanoparticles.

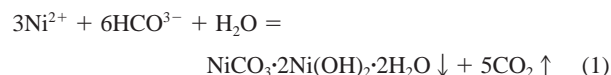
In recent years, the coating process with nanoparticles has been investigated for fabricating homogeneous ceramics. The process improves not only the sintering activity and densification,<sup>9</sup> but also the different phase uniformity and mechanical properties of the sintered body.<sup>10</sup> Several methods are introduced to prepare the coated powders, such as coprecipitation,<sup>11</sup> sol-gel,<sup>12</sup> and electroless plating.<sup>13</sup> Coprecipitation is the most promising way, owing to

the relatively low cost of the reactants and easily controlled fabrication process. However, there is no report on the fabrication of nanoparticle-coated PZT powders using this method.

In the present study, PZT powders coated with NiO nanoparticles are fabricated by the heterogeneous precipitation method. The microstructure of the coated powders is investigated in detail. The purpose of this study is to obtain much better microstructure and high-performance PZT/NiO nanocomposites.

## II. Experimental Procedures

The coated PZT powders were prepared using PZT powders with the diameter of 0.36 μm (self-made), Ni(NO<sub>3</sub>)<sub>2</sub>·6H<sub>2</sub>O (analytically) and NH<sub>4</sub>HCO<sub>3</sub> (analytically) as starting materials. PZT powders, Ni(NO<sub>3</sub>)<sub>2</sub>·6H<sub>2</sub>O solution of 1.0M (corresponding to 0.9–7.4 vol% NiO in the final coated powders) and polyacrylic acid (1.0 wt% of PZT weight) as dispersant were mixed in a polyethylene pot for 24 h using distilled water and ZrO<sub>2</sub> balls as the grinding medium. Then, NH<sub>4</sub>HCO<sub>3</sub> solution of 1.0M was added dropwise to the homogeneous slurry obtained above under vigorous stirring. The reaction is shown in the following equation:<sup>14</sup>



To ensure completion of the reaction, an excess of NH<sub>4</sub>HCO<sub>3</sub> was added to the slurry and the pH value of the mixture was ~7–8. Finally, the obtained precipitates were thoroughly washed with distilled water and ethanol and dried at 60°C in an oven. The dried precipitates were calcined at 400°C for 2 h in air. To investigate the characteristic microstructure of the NiO nanoparticle-coated PZT powders in more detail, the 7.4 vol% NiO-coated PZT powders were selected to study.

The NiO content of coated powders was determined by inductively coupled plasma atomic emission spectrometry (ICP-AES; Varian Vista AX, Palo Alto, CA). The thermal decomposition behavior of as-precipitated powders was analyzed by thermogravimetry (TG) and differential scanning calorimetry (DSC) on an automated thermal analyzer (Model STA 449C, Netzsch, Exton, PA). DSC-TG analysis was conducted in air at a heating rate of 10°C/min from room temperature to 600°C. Transmission electron microscopy (TEM) with energy dispersive spectroscopy (EDS; Model JEM-200CX, JEOL, Tokyo, Japan) was applied to investigate the microstructure of the coated powders. SAD pattern was used to identify the crystallinity of the coated powders. For powder-phase characterization, an XRD pattern was obtained using automated diffractometry (Model RAX-10, Rigaku, Tokyo, Japan) with CuK<sub>α1</sub> radiation.

## III. Results and Discussion

DSC and TG curves of as-precipitated powders are shown in Fig. 1. There are two major weight losses indicated in the TG curve. The first major weight loss from room temperature to

W.A. Schulze—contributing editor

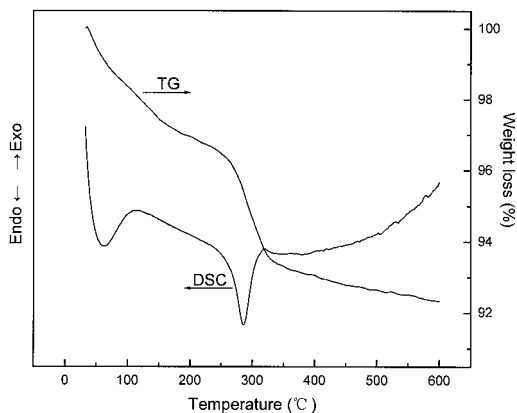


Fig. 1. DSC and TG curves of the as-precipitated PZT powders.

115°C is attributed to the desorption of physically absorbed water and ethanol and the removal of crystalline water. This is supported by an endothermic peak at 65°C on the DSC curve. The temperature of endothermic peak is lower than the boiling point of water, indicating that the elimination of crystalline water of precipitate ( $\text{NiCO}_3 \cdot 2\text{Ni}(\text{OH})_2 \cdot 2\text{H}_2\text{O}$ ) contributes more to the weight loss. The other major weight loss from 240°–320°C on the TG curve is due to decomposition of the precipitate together with the removal of the organic compounds, which coincides with the endothermic peak at 285°C. According to DSC-TG analysis, the calcination of as-precipitated powder is conducted at 400°C for 2 h to ensure the complete decomposition of the precipitate ( $\text{NiCO}_3 \cdot 2\text{Ni}(\text{OH})_2 \cdot 2\text{H}_2\text{O}$ ).

Figure 2(a) shows the TEM image of uncoated PZT powders. It can be seen that the PZT particles have relatively smooth and dense surfaces. There are no other particle adhering to the surface of PZT particles. A TEM image of coated PZT powders obtained by precipitation is shown in Fig. 2(b). There is a uniform coating on the surface of PZT particles in Fig. 2(b). The EDS of the coated particles shows that the peak intensity ratio of nickel to lead at the edge field (Fig. 3(a)) is much higher

than that in the center field (Fig. 3(b)). The presence of carbon is attributed primarily to the precipitates adhering to the surface of PZT particles. This is a typical coated structure. The core is a PZT particle and the coating layer is  $\text{NiCO}_3 \cdot 2\text{Ni}(\text{OH})_2 \cdot 2\text{H}_2\text{O}$ . These observations suggest that the nuclei of  $\text{NiCO}_3 \cdot 2\text{Ni}(\text{OH})_2 \cdot 2\text{H}_2\text{O}$  in the slurry grow on the surface of a PZT core particle instead of forming discrete precipitates in the presence of ultrafine PZT powders. The surface of PZT particle serves as the heterogeneous nucleation site. The TEM image and SAD pattern of the coated PZT powders calcined at 400°C for 2 h are shown in Fig. 4. It is evident that the precipitates decompose to nanoparticles in the coating layer with a thickness of ~30 nm on the surface of PZT particle. The TEM image (Fig. 4(b)) shows that the nanoparticles with an average size of ~8 nm are spherical and weakly agglomerated.

The phase characterization of the coating layers on the surface of PZT cannot be identified from the XRD analysis patterns of the coated PZT powders before (Fig. 5(b)) and after calcination (Fig. 5(c)). To verify the phase coating layers, another sample was prepared using  $\text{Ni}(\text{NO}_3)_2 \cdot 6\text{H}_2\text{O}$  and  $\text{NH}_4\text{HCO}_3$  as starting materials by the same process without the presence of PZT powders. The XRD analysis results (Figs. 5(d) and 5(e)) indicate that the precipitate  $\text{NiCO}_3 \cdot 2\text{Ni}(\text{OH})_2 \cdot 2\text{H}_2\text{O}$  is an amorphous phase that decomposes to NiO with cubic phase after calcining at 400°C for 2 h. No new diffraction peaks appear except for PZT in Fig. 5(b) because the coating layer is amorphous phase. No obvious new diffraction peaks appear on the XRD patterns of the calcined powders because the two relatively strong peaks (111) and (200) of cubic NiO are overlapped by the peaks (111) and (002) of tetragonal PZT, respectively. Based on the XRD analysis, it can be concluded that the amorphous coating layer on the surface of PZT particle is crystallized to NiO with cubic phase after calcination. The SAD pattern of the coated powders after calcination (Fig. 4(c)) further confirms this conclusion. There are two sets of diffraction patterns in NiO-coated PZT powders, the spots and the ring patterns corresponding to PZT crystal and NiO polycrystal, respectively. The diffraction ring patterns also reveal that the nano-sized particles are NiO with cubic phase.

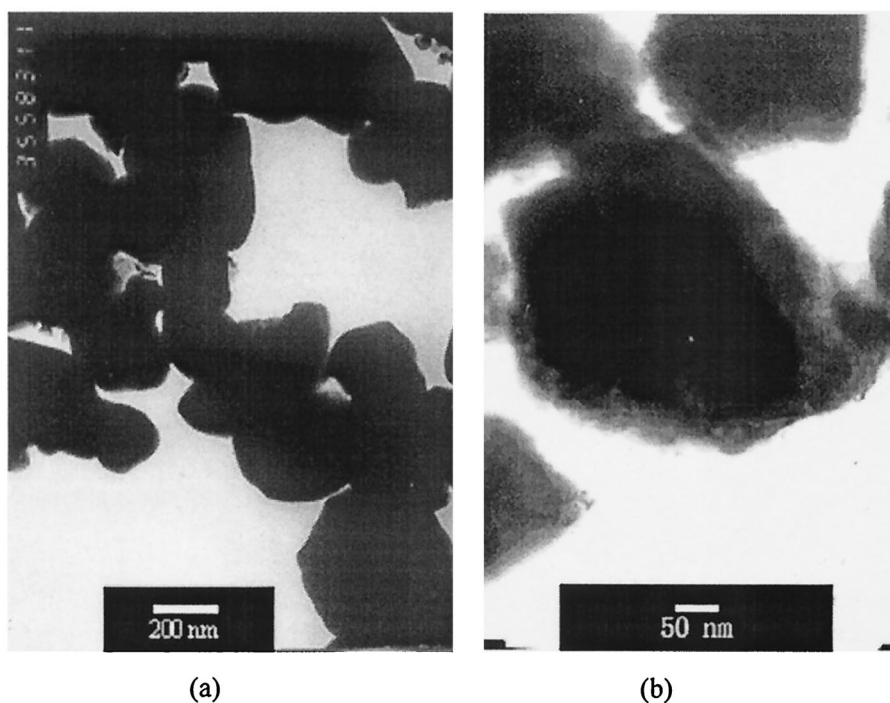
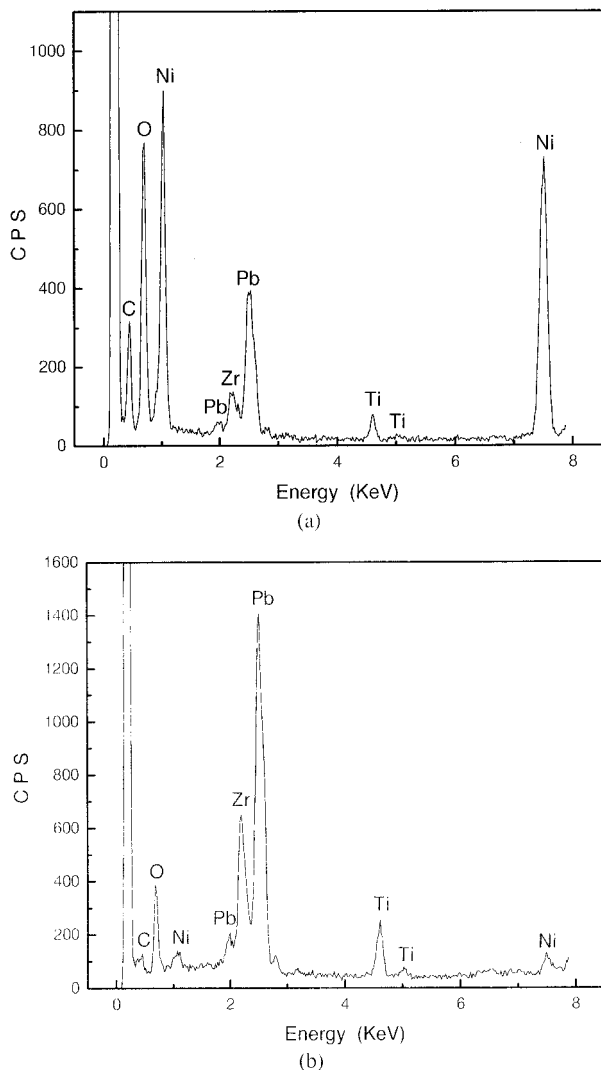


Fig. 2. TEM images of (a) the uncoated PZT powders and (b) the coated (as-precipitated) PZT powders.



**Fig. 3.** EDS spectra of the coated (as-precipitated) PZT particle (a) at the edge field and (b) in the center field.

### III. Conclusions

Weakly agglomerated NiO nanoparticles are successfully coated on the surface of PZT particles by the heterogeneous precipitation

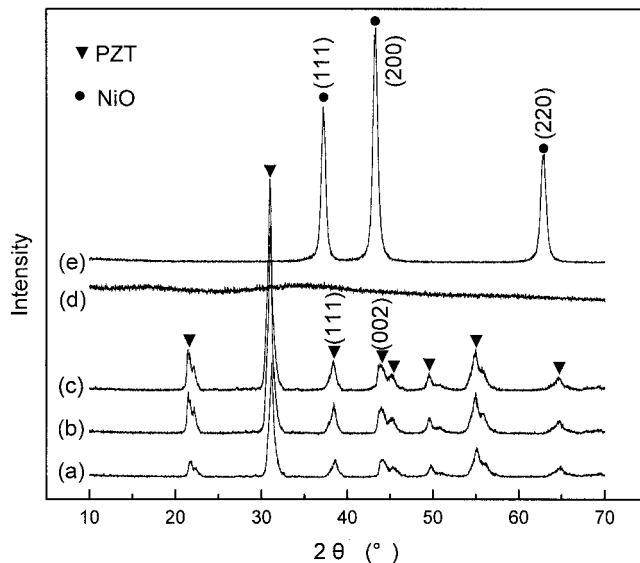


**Fig. 5.** XRD patterns of (a) uncoated PZT powders, (b) coated (as-precipitated) PZT powders, (c) coated PZT powders calcined at 400°C for 2 h, (d) precipitates without the presence of PZT, and (e) precipitates without the presence of PZT calcined at 400°C for 2 h.

method. The surface of the PZT particle serves as the heterogeneous nucleation site and the nuclei of  $\text{NiCO}_3 \cdot 2\text{Ni}(\text{OH})_2 \cdot 2\text{H}_2\text{O}$  in the slurry grow on the surface of particles instead of forming discrete precipitates. The spherical NiO particles with the size of  $\sim 8$  nm are obtained by calcining the coated powders at 400°C for 2 h. The thickness of the coating layer of nanocrystalline NiO is  $\sim 30$  nm.

### References

- S. R. Winzer, N. Shankar, and A. P. Ritter, "Designing Cofired Multilayer Electrostrictive Actuator for Reliability," *J. Am. Ceram. Soc.*, **72**, 2246–57 (1989).
- G. S. White, A. S. Raynes, M. D. Vaudin, and S. W. Freiman, "Fracture Behavior of Cyclically Loaded PZT," *J. Am. Ceram. Soc.*, **77**, 2603–608 (1994).
- H. J. Hwang, K. Tajima, M. Sando, M. Toriyama, and K. Niihara, "Fatigue Behavior of PZT-Based Nanocomposites with Fine Platinum Particles," *J. Am. Ceram. Soc.*, **81**, 3325–28 (1998).
- H. J. Hwang, M. Yasuoka, M. Sando, and M. Toriyama, "Fabrication, Sinterability, and Mechanical Properties of Lead Zirconate Titanate/Silver Composites," *J. Am. Ceram. Soc.*, **82**, 2417–22 (1999).
- K. Tajima, H. J. Hwang, M. Sando, and K. Niihara, "PZT Nanocomposites Reinforced by Small Amount of Oxides," *J. Eur. Ceram. Soc.*, **19**, 345–51 (1999).

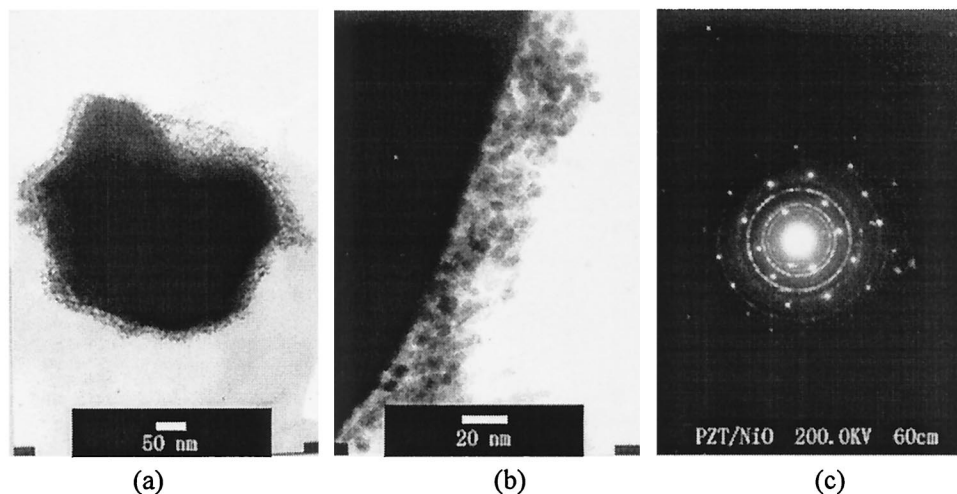


**Fig. 4.** TEM images ((a) and (b)) and corresponding SAD pattern of the coated PZT powders calcined at 400°C for 2 h.

<sup>6</sup>K. Tajima, H. J. Hwang, and M. Sando, "Electric-Field-Induced Crack Growth Behavior in PZT/Al<sub>2</sub>O<sub>3</sub> Composites," *J. Am. Ceram. Soc.*, **83**, 651–53 (2000).

<sup>7</sup>K. Niihara, "New Design Concept of Structural Ceramics-Ceramics Nanocomposites," *J. Ceram. Soc. Jpn.*, **99**, 974–82 (1991).

<sup>8</sup>T. Ohji, Y. K. Jeong, Y. H. Choa, and K. Niihara, "Strengthening and Toughening Mechanisms of Ceramic Nanocomposites," *J. Am. Ceram. Soc.*, **81**, 1453–60 (1998).

<sup>9</sup>C. M. Wang and F. L. Riley, "Alumina-Coating of Silicon Nitride Powder," *J. Eur. Ceram. Soc.*, **10**, 82–93 (1992).

<sup>10</sup>W. H. Tuan, H. H. Wu, and T. J. Yang, "The Preparation of Al<sub>2</sub>O<sub>3</sub>/Ni Composites by a Powder Coating Technique," *J. Mater. Sci.*, **30**, 855–59 (1995).

<sup>11</sup>D. Kopolnek and C. De Jonghe, "Particulate Composites from Coated Powders," *J. Eur. Ceram. Soc.*, **7**, 345–51 (1991).

<sup>12</sup>C. Y. Yang and W. H. Shih, "Effect of Acid on the Coating of Boehmite onto Silicon Carbide Particles in Aqueous Suspensions," *J. Am. Ceram. Soc.*, **82**, 436–40 (1999).

<sup>13</sup>H. J. Hwang, K. Tajima, M. Sando, M. Toriyama, and K. Niihara, "Microstructure and Mechanical Properties of Lead Zirconate Titanate (PZT) Nanocomposites with Platinum Particles," *J. Ceram. Soc. Jpn.*, **108**, 339–44 (2000).

<sup>14</sup>Y. Li, C. Li, X. Duan, H. Zheng, L. Li, Y. Qian, "Preparation of Nanocrystalline NiO in Mixed Solvent," *Journal of China University of Science and Technology*, **27**, 346–49 (1997). □